Vol 18 No 10, October 2009
1674-1056/2009/18(10)/4393–14

Chinese Physics B

© 2009 Chin. Phys. Soc.
and IOP Publishing Ltd

Discrete gap breathers in a two-dimensional diatomic face-centered square lattice*

Lü Bin-Bin(吕彬彬)† and Tian Qiang(田 强)

Department of Physics, Beijing Normal University, Beijing 100875, *China*

(Received 4 January 2009; revised manuscript received 20 May 2009)

In this paper we study the existence and stability of two-dimensional discrete gap breathers in a two-dimensional diatomic face-centered square lattice consisting of alternating light and heavy atoms, with on-site potential and coupling potential. This study is focused on two-dimensional breathers with their frequency in the gap that separates the acoustic and optical bands of the phonon spectrum. We demonstrate the possibility of the existence of two-dimensional gap breathers by using a numerical method. Six types of two-dimensional gap breathers are obtained, i.e., symmetric, mirror-symmetric and asymmetric, whether the center of the breather is on a light or a heavy atom. The difference between one-dimensional discrete gap breathers and two-dimensional discrete gap breathers is also discussed. We use Aubry's theory to analyze the stability of discrete gap breathers in the two-dimensional diatomic face-centered square lattice.

Keywords: discrete gap breathers, two-dimensional diatomic face-centered square lattice, linear stability, coupling parameters

PACC: 6320R, 6320P, 0547

1. Introduction

Since the discovery of intrinsic localized modes (ILMs) or discrete breathers (DBs) in Klein–Gordon (KG) and Fermi–Pasta–Ulam (FPU) lattices in the late 1980s,[1,2] DBs and solitons have been a topic of increasing interest in view of their significant role in energy localization and transport. In 1994, Mackay and Aubry established the existence of stationary breathers in a broad range of lattice models.[3] In their method, breathers are obtained by continuation from the anticontinuum limit at which the network is reduced to an array of uncoupled oscillators. Soon afterwards, the conditions for the existence of breathers with a frequency above the optical band and inside the gap separating it from the acoustic one were presented by Cretegny, Livi and Spicci.[4] In 2003, Maniadis, Zolotaryuk and Tsironis gave the four cases of discrete gap breathers (DGBs).[5] The proof of the existence of breathers in diatomic FPU chains with arbitrary mass ratio was presented by James and Noble.[6] Because the discrete breathers' dynamics are similar to impurity modes that can move in gap, the DGBs, as a kind of localized modes in one-dimensional (1D) diatomic Klein–Gordon chain,[7] in 1D mixed Klein–Gordon/Fermi–Pasta–Ulam chain[8] and in 1D diatomic β-FPU chain, its local characteristic and stability were presented by Lü and Tian.[9,10] All of them focused on the 1D diatomic system. Recently, the DBs in the two-dimensional (2D) diatomic square lattice are increasingly catching people's interest. Butt and Wattis,[11] Bao and Takuji,[12] investigated the 2D monatomic FPU system.

The purpose of this paper is to investigate the possibility of the existence and stability of the DGBs in a 2D diatomic face-centered square lattice. First, we discuss the DGBs in a 1D diatomic chain and analyze the effects of different system parameters on DGBs. Secondly, by controlling different system parameters, we transform a general 2D diatomic model into the 2D KG model or the 2D β-FPU model. Thirdly, in terms of the harmonic approximation, we discuss the linearly dispersive relation of the phonon in the lattice. Fourthly, we prove the existence of the 2D DGBs in a 2D diatomic face-centered square lattice by using the rotating wave approximation (RWA),[5] the local anharmonicity approximation (LAA)[5] and

*Project supported by the National Natural Science Foundation of China (Grant No 10574011), and the Foundation for Researching Group by Beijing Normal University.

†Corresponding author. E-mail: lbbsuccess@126.com

the numerical method, and obtained six types of 2D DGBs, i.e., symmetric, mirror-symmetric and asymmetric, whether the center of the breather is on a light or a heavy atom. The stability of discrete periodic solution of discrete nonlinear system has been discussed in many papers.[13−18] According to Aubry's theory,[16,17] we analyse the stability of DGBs in the 2D diatomic face-centered square lattice.

2. The one-dimensional model

We consider a generalised discrete 1D diatomic chain model, the Hamiltonian of the system is given by

$$\begin{aligned} H &= \sum_s \left[\frac{\dot{u}_{2s}^2}{2M_1} + \frac{\dot{u}_{2s+1}^2}{2M_2} + \frac{1}{2}\omega_0^2 u_{2s}^2 + \frac{1}{2}\omega_0^2 u_{2s+1}^2 \right. \\ &+ \frac{1}{3}\kappa u_{2s}^3 + \frac{1}{3}\kappa u_{2s+1}^3 + \frac{1}{4}\gamma u_{2s}^4 + \frac{1}{4}\gamma u_{2s+1}^4 \\ &+ \frac{1}{2}k_2 \left(u_{2s} - u_{2s+1}\right)^2 + \frac{1}{2}k_2 \left(u_{2s+1} - u_{2s+2}\right)^2 \\ &+ \frac{1}{3}\alpha \left(u_{2s} - u_{2s+1}\right)^3 + \frac{1}{3}\alpha \left(u_{2s+1} - u_{2s+2}\right)^3 \\ &+ \left. \frac{1}{4}\beta \left(u_{2s} - u_{2s-1}\right)^4 + \frac{1}{4}\beta \left(u_{2s+1} - u_{2s+2}\right)^4 \right]. \quad (1) \end{aligned}$$

2.1. The discrete gap breathers in a 1D β-FPU diatomic chain

When $\omega_0 = \kappa = \gamma = \alpha = 0$, the model is the 1D β-FPU diatomic chain, the Hamiltonian of it is given by

$$\begin{aligned} H = &\sum_s \frac{1}{2}M_1 \dot{u}_{2s}^2 + \frac{1}{2}M_2 \dot{u}_{2s+1}^2 + W(u_{2s} - u_{2s+1}) \\ &+ W(u_{2s+1} - u_{2s+2}) \end{aligned} \quad (2)$$

with $W(r)$ being the interaction potential

$$W(r) = \frac{k_2}{2}r^2 + \frac{\beta}{4}r^4 \ , \quad (3)$$

where M_1 and M_2 are the masses of the heavy and light atoms, u_{2s} and u_{2s+1} are the displacements of the heavy and light atoms in the $2s$-th and $(2s+1)$-th cells of the lattice from their equilibriums, k_2 and β are the linear coupling parameter and nonlinear coupling parameter, respectively. The nonlinear vibration equations for this system are given as follows:

$$\begin{aligned} &M_1 \ddot{u}_{2s} \\ &= k_2(u_{2s+1} - 2u_{2s} + u_{2s-1}) \\ &\quad + \beta[(u_{2s+1} - u_{2s})^3 - (u_{2s} - u_{2s-1})^3] \ , \end{aligned} \quad (4)$$

$$\begin{aligned} &M_2 \ddot{u}_{2s+1} \\ &= k_2(u_{2s+2} - 2u_{2s+1} + u_{2s}) \\ &\quad + \beta[(u_{2s+2} - u_{2s+1})^3 - (u_{2s+1} - u_{2s})^3] \ . \end{aligned} \quad (5)$$

In the 1D system, we only consider the nearest neighbour interactions. As in numerical calculation, a necessary condition for the breather to exist is to avoid resonances with the phonons. This means that the breather frequency and all its higher harmonic must lie outside the phonon bands, but the frequency can lie inside the gap or above the optical band. Here, we only focus on the case that it lies inside the gap. For this, we introduce the LAA and RWA, then, we still assume the 1D DGBs to be of the following type

$$u_n(t) = u_n^0 \cos \omega t \ . \quad (6)$$

Substituting Eq.(6) into Eqs.(4) and (5), then they can be rewritten as follows:

$$\begin{aligned} &\omega_b \left(\omega_b + \frac{2}{\sqrt{\gamma} - 1}\right) v_{2s}^0 + C(v_{2s+1}^0 + v_{2s-1}^0) \\ &+ \frac{gC}{2}[(v_{2s+1}^0 - v_{2s}^0)^3 - (v_{2s}^0 - v_{2s-1}^0)^3] = 0, \end{aligned} \quad (7)$$

$$\begin{aligned} &(\omega_b - 1) \left(\omega_b + \frac{\sqrt{\gamma} + 1}{\sqrt{\gamma} - 1}\right) v_{2s+1}^0 + \gamma C(v_{2s+2}^0 + v_{2s}^0) \\ &+ \frac{gC\gamma}{2}[(v_{2s+2}^0 - v_{2s+1}^0)^3 - (v_{2s+1}^0 - v_{2s}^0)^3] = 0. \end{aligned} \quad (8)$$

In the above analysis, $v_n^0 = \dfrac{u_n^0}{a}$, $\gamma = \dfrac{M_1}{M_2}$, $C = \dfrac{1}{(\sqrt{\gamma} - 1)^2(2 + gv_0')}$, $g = \dfrac{\beta a^2}{k_2}$, and ω_b is the frequency of the DGB. Maniadis, Zolotaryuk and Tsironis[5] have gave four types of DGBs in 1D β-FPU diatomic chain. The four DGBs are light-particle symmetric, heavy-particle symmetric, light-particle antisymmetric, heavy-particle antisymmetric (LS, HS, LA, HA). In the following section, we will discuss the effect of different system parameters on the localization of DGBs, we only select the HS as an example to analyse.

(i) The effect of different mass ratio on the stability of DGBs (HS)

From the numerical results of Fig.1, we obtain that the 1D DGBs profiles are correlated closely to the mass ratio, i.e., the larger the mass ratio, the better the localization of the 1D DGBs profiles. This is because the interaction of the nearest-neighbour atoms in the 1D diatomic FPU models becomes weaker when the mass ratio increases.

(ii) The effect of the hard coupling potential on the localization of DGBs (HS)

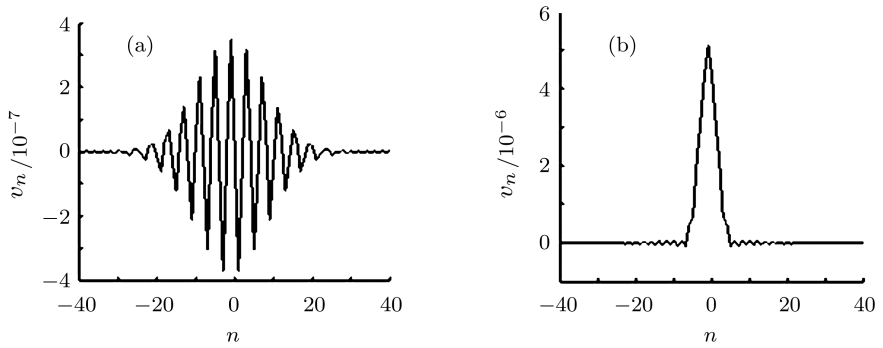


Fig.1. The graphical illustration of the effect of different mass ratio on the stability of DGBs (a) $M_1/M_2 = 2$, (b) $M_1/M_2 = 16$.

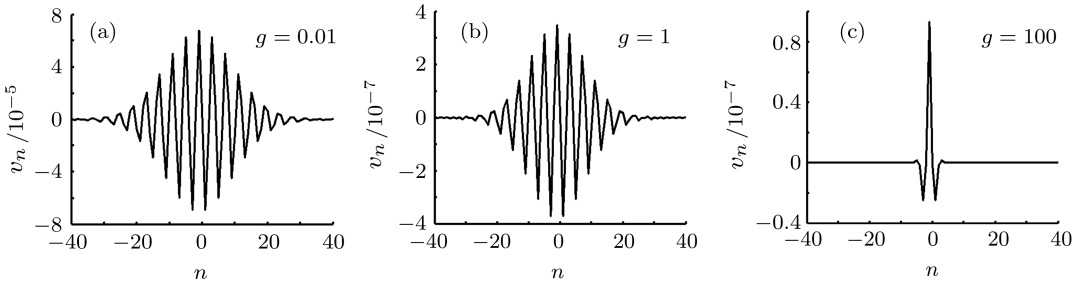


Fig.2. The graphical illustration of the localization of DGBs as a function of nonlinear coupling potential: (a) the hard quartic nonlinear coupling potential with $g = 0.01$; (b) the hard quartic nonlinear coupling potential with $g = 1$; (c) the hard quartic nonlinear coupling potential with $g = 100$.

From the numerical results of Fig.2, we obtain that the 1D DGBs profiles are correlated closely with the quartic nonlinear coupling parameter.

(iii) The effect of the soft coupling potential on the localization of DGBs (HS)

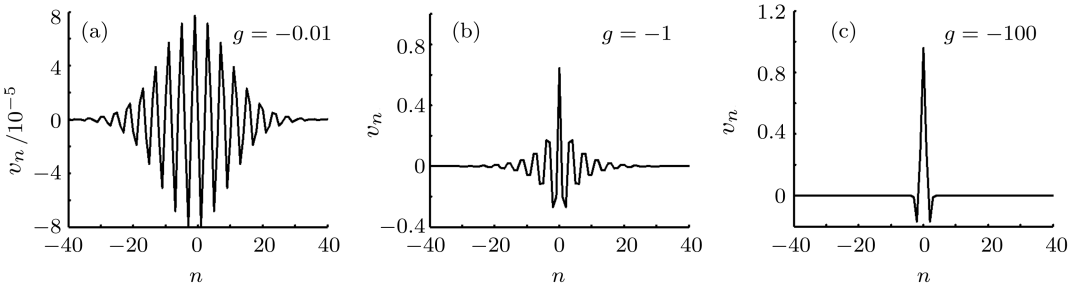


Fig.3. The graphical illustration of the profiles of the effect of different nonlinear coupling potentials: (a) soft coupling potential with $g = -0.01$ and mass ratio $M_1/M_2 = 2$; (b) soft coupling potential with $g = -1$ and mass ratio $M_1/M_2 = 2$; (c) soft coupling potential with $g = -100$ and mass ratio $M_1/M_2 = 2$.

In a 1D FPU model, the nonlinear coupling parameters $\beta > 0$ is the hard coupling potential, and otherwise is soft coupling potential. We have investigated the relation between the coupling potential and localization. Figures 2 and 3 show that under the soft coupling potential, the localization of the 2D DGBs profiles is better than that under the hard coupling potential. Also, the larger the nonlinear coupling parameters, the larger the amplitudes of the 1D DGBs.

2.2. The discrete gap breathers in a 1D KG diatomic chain

For $\kappa = \alpha = \beta = 0$, the general Hamiltonian (1) is transformed into the 1D KG diatomic chain

$$H = \sum_s \left[\frac{\dot{u}_{2s}^2}{2M_1} + \frac{\dot{u}_{2s+1}^2}{2M_2} + \frac{1}{2}\omega_0^2 u_{2s}^2 + \frac{1}{2}\omega_0^2 u_{2s+1}^2 + \frac{1}{4}\gamma u_{2s}^4 + \frac{1}{4}\gamma u_{2s+1}^4 + \frac{1}{2}k_2 \left(u_{2s} - u_{2s+1}\right)^2 + \frac{1}{2}k_2 \left(u_{2s+1} - u_{2s+2}\right)^2 \right], \quad (9)$$

where M_1 and M_2 are the masses of the heavy and light atoms, u_{2s} and u_{2s+1} are the displacements of the heavy and light atoms in the $2s$-th and $(2s+1)$-th cell of the lattice from their equilibrium points, respectively, ω_0 and β are the on-site potential parameters; k_2 is the linear coupling parameter. Applying the same numerical methods as in 1D FPU model, we see that, in a 1D KG model, there are also four types of DGBs which are the same as in the 1D FPU model. In a 1D KG chain, the larger the mass ratio, the better the localization of the 1D DGBs profiles; and the larger the onsite potential parameters, the larger the amplitudes of the 1D DGBs.

3. The two-dimensional model

The Hamiltonian of a general 2D diatomic face-centered square lattice is given by

$$\begin{aligned} H = & \sum_{m,n} \left[\frac{\dot{u}_{2m-1,2n-1}^2}{2M_1} + \frac{\dot{u}_{2m,2n}^2}{2M_2} + \frac{1}{2}\omega_0^2 u_{2m-1,2n-1}^2 + \frac{1}{2}\omega_0^2 u_{2m,2n}^2 + \frac{1}{3}\kappa u_{2m-1,2n-1}^3 + \frac{1}{3}\kappa u_{2m,2n}^3 + \frac{1}{4}\gamma u_{2m,2n}^4 \right. \\ & + \frac{1}{4}\gamma u_{2m-1,2n-1}^4 + \frac{1}{2}C \left(u_{2m,2n} - u_{2m-1,2n-1}\right)^2 + \frac{1}{2}C \left(u_{2m+1,2n+1} - u_{2m,2n}\right)^2 + \frac{1}{3}\alpha \left(u_{2m,2n} - u_{2m-1,2n-1}\right)^3 \\ & \left. + \frac{1}{3}\alpha \left(u_{2m+1,2n+1} - u_{2m,2n}\right)^3 + \frac{1}{4}\beta \left(u_{2m,2n} - u_{2m-1,2n-1}\right)^4 + \frac{1}{4}\beta \left(u_{2m+1,2n+1} - u_{2m,2n}\right)^4 \right]. \end{aligned} \quad (10)$$

3.1. The discrete gap breathers in a 2D KG diatomic face-centered square lattice

For $\kappa = \alpha = \beta = 0$, the general Hamiltonian (10) is transformed into that for the 2D KG diatomic face-centered square lattice

$$\begin{aligned} H = & \sum_{m,n} \left[\frac{\dot{u}_{2m-1,2n-1}^2}{2M_1} + \frac{\dot{u}_{2m,2n}^2}{2M_2} + \frac{1}{2}\omega_0^2 u_{2m-1,2n-1}^2 + \frac{1}{2}\omega_0^2 u_{2m,2n}^2 + \frac{1}{4}\gamma u_{2m,2n}^4 + \frac{1}{4}\gamma u_{2m-1,2n-1}^4 \right. \\ & \left. + \frac{1}{2}C \left(u_{2m,2n} - u_{2m-1,2n-1}\right)^2 + \frac{1}{2}C \left(u_{2m+1,2n+1} - u_{2m,2n}\right)^2 \right], \end{aligned} \quad (11)$$

where M_1 and M_2 are the masses of the heavy and light atoms, $u_{2m-1,2n-1}$ and $u_{2m,2n}$ are the displacements of the heavy and light atoms in the (m,n)-th cell of the lattice from their equilibrium points, ω_0 and β are the on-site potential parameters, C is the linear coupling parameter. The nonlinear vibration equations for this system are obtained as follows:

$$\begin{aligned} & M_1 \ddot{u}_{2m-1,2n-1} \\ = & -\omega_0^2 u_{2m-1,2n-1} - \gamma u_{2m-1,2n-1}^3 + C \left(u_{2m,2n} + u_{2m-2,2n-2} + u_{2m-2,2n} + u_{2m,2n-2} - 4u_{2m-1,2n-1}\right), \end{aligned} \quad (12)$$

$$\begin{aligned} & M_2 \ddot{u}_{2m,2n} \\ = & -\omega_0^2 u_{2m,2n} - \gamma u_{2m,2n}^3 + C \left(u_{2m+1,2n+1} + u_{2m-1,2n-1} + u_{2m-1,2n+1} + u_{2m+1,2n-1} - 4u_{2m,2n}\right). \end{aligned} \quad (13)$$

Under harmonic approximation, the vibration equations for this system is obtained as follows:

$$M_1 \ddot{u}_{2m-1,2n-1} = -\omega_0^2 u_{2m-1,2n-1} + C \left(u_{2m,2n} + u_{2m-2,2n-2} + u_{2m-2,2n} + u_{2m,2n-2} - 4u_{2m-1,2n-1}\right), \quad (14)$$

$$M_2 \ddot{u}_{2m,2n} = -\omega_0^2 u_{2m,2n} + C \left(u_{2m+1,2n+1} + u_{2m-1,2n-1} + u_{2m-1,2n+1} + u_{2m+1,2n-1} - 4u_{2m,2n}\right). \quad (15)$$

The linearly dispersive relation of the phonon in the lattice reads

$$\omega_{\pm}^2 = \frac{1}{2}\left\{\frac{2C+\omega_0}{M_2}+\frac{2C+\omega_0}{M_1} \pm \left[\left(\frac{2C+\omega_0}{M_2}-\frac{2C+\omega_0}{M_1}\right)^2+\frac{16C^2\cos^2(2qa_0)}{M_1M_2}\right]^{1/2}\right\}. \tag{16}$$

We define the edges of these bands by $\omega_{1,}\quad \omega_{2,}\ \omega_3$ and ω_4, thus we have

$$\begin{aligned}&\omega_1 = 0,\quad (q\to 0)\,,\quad \omega_2 = \sqrt{\frac{2C}{M_1}},\quad \left(q=\pm\frac{\pi}{4a_0}\right),\\ &\omega_3 = \sqrt{\frac{2C}{M_2}},\quad \left(q=\pm\frac{\pi}{4a_0}\right),\quad \omega_4 = \sqrt{\frac{2C}{\mu}},\quad (q\to 0)\,,\end{aligned} \tag{17}$$

where $\mu = M_1M_2/(M_1+M_2)$ and $M_1 > M_2$. The acoustic band has frequencies lying between ω_1 and ω_2, and the optical one has the frequencies lying between ω_3 and ω_4. We call ω_2 and ω_3 the lower and the upper edges of the phonon band gap, respectively. Substituting Eq.(17) into Eq.(16), we obtain the linearly dispersive relation of the phonon in the lattice

$$\begin{aligned}&\omega_{\pm}^2\\ &= \frac{1}{2}\{\omega_4^2+\Omega_{M_2}^2+\Omega_{M_1}^2 \pm [(\omega_3^2-\omega_2^2+\Omega_{M_2}^2-\Omega_{M_1}^2)^2\\ &\quad + 4\omega_3^2\omega_2^2\cos^2(2qa_0)]^{1/2}\},\end{aligned} \tag{18}$$

where $\Omega_{M_2} = \sqrt{\omega_0^2/M_2}$ and $\Omega_{M_1} = \sqrt{\omega_0^2/M_1}$ are the frequencies of discrete light atoms and heavy atoms, respectively. At the edge of Brillouin zone $q_{\rm B} = \pm\pi/4a_0$, we have

$$\omega_{\pm}(q_{\rm B})^2 = \begin{cases}\omega_3^2+\Omega_{M_2}^2 = \dfrac{2C+\omega_0^2}{M_2},\\ \omega_2^2+\Omega_{M_1}^2 = \dfrac{2C+\omega_0^2}{M_1}.\end{cases} \tag{19}$$

Because of the existence of on-site potential, the acoustic and optical phonon bands have been raised. The band gap is

$$\begin{aligned}\omega_{\rm gap} &= \omega_+(q_{\rm B})-\omega_-(q_{\rm B})\\ &= \left(\sqrt{\frac{M_1}{M_2}}-1\right)\omega_-(q_{\rm B}).\end{aligned} \tag{20}$$

At the center of Brillouin zone $q=0$, we have

$$\begin{aligned}&\omega_{\pm}^2(0)\\ &= \frac{1}{2}\{\omega_4^2+\Omega_{M_2}^2+\Omega_{M_1}^2 \pm [(\omega_3^2-\omega_2^2+\Omega_{M_2}^2-\Omega_{M_1}^2)^2\\ &\quad + 4\omega_3^2\omega_2^2]^{1/2}\}.\end{aligned} \tag{21}$$

From the above result, we know $\omega_-(0)\neq 0$. So there is a band gap, which is the obvious feature of the dispersive relation under the existence of on-site potential.

In the above analysis, we consider only the nearest-neighbour interaction. In a 2D system, the second nearest-neighbour interaction is very important for the stability of the system. In the following, we shall analyse the stability of the 2D DGBs by considering the nearest-neighbour and the second nearest-neighbour interactions. The nonlinear vibration equation for this system is obtained as follows:

$$\begin{aligned}&M_1\ddot{u}_{2m-1,2n-1}\\ &= -\omega_0^2u_{2m-1,2n-1}-\gamma u_{2m-1,2n-1}^3+C\left(u_{2m,2n}+u_{2m-2,2n-2}+u_{2m,2n-2}+u_{2m-2,2n}-4u_{2m-1,2n-1}\right)\\ &\quad + C\left(u_{2m-1,2n+1}+u_{2m-1,2n-3}+u_{2m+1,2n-1}+u_{2m-3,2n-1}-4u_{2m-1,2n-1}\right),\end{aligned} \tag{22}$$

$$\begin{aligned}&M_2\ddot{u}_{2m,2n}\\ &= -\omega_0^2u_{2m,2n}-\gamma u_{2m,2n}^3+C\left(u_{2m+1,2n+1}+u_{2m-1,2n-1}+u_{2m+1,2n-1}+u_{2m-1,2n+1}-4u_{2m,2n}\right)\\ &\quad + C\left(u_{2m,2n+2}+u_{2m,2n-2}+u_{2m+2,2n}+u_{2m-2,2n}-4u_{2m,2n}\right).\end{aligned} \tag{23}$$

In numerical calculation, a necessary condition for the breather to exist is to avoid resonances with the phonons, i.e., the breather frequency and all its higher harmonics must lie outside the phonon bands. The frequency can lie inside the gap or above the optical band. Here, we only focused on the case with the frequency lying inside the gap. For this, we introduce the LAA and RWA, and assume the 2D DGBs to be of the following types,

$$u_{2m-1,2n-1}(t) = u^0_{2m-1,2n-1}\cos\omega t,$$
$$u_{2m,2n}(t) = u^0_{2m,2n}\cos\omega t. \tag{24}$$

Substituting Eq.(24) into Eqs.(22) and (23). Equations (22) and (23) can be rewritten as follows:

$$\left(\frac{\omega^2-\omega_-^2(q_{\rm B})}{\omega_2^2}-1\right)u^0_{2m-1,2n-1}+\frac{1}{2}\left(u^0_{2m,2n}+u^0_{2m-2,2n}+u^0_{2m-2,2n-2}+u^0_{2m,2n-2}-2u^0_{2m-1,2n-1}\right)$$
$$+\frac{1}{2}\left(u^0_{2m-1,2n+1}+u^0_{2m+1,2n-1}+u^0_{2m-1,2n-3}+u^0_{2m-3,2n-1}-2u^0_{2m-1,2n-1}\right)-\frac{\gamma}{4C}(u^0_{2m-1,2n-1})^3=0, \tag{25}$$
$$\left(\frac{\omega^2-\omega_+^2(q_{\rm B})}{\omega_3^2}-1\right)u^0_{2m,2n}+\frac{1}{2}\left(u^0_{2m+1,2n+1}+u^0_{2m-1,2n-1}+u^0_{2m-1,2n+1}+u^0_{2m+1,2n-1}-2u^0_{2m,2n}\right)$$
$$+\frac{1}{2}\left(u^0_{2m-2,2}+u^0_{2m,2n-2}+u^0_{2m+2,2n}+u^0_{2m,2n+2}-2u^0_{2m,2n}\right)-\frac{\gamma}{4C}(u^0_{2m,2n})^3=0. \tag{26}$$

The numerical solutions of Eqs.(25) and (26) are shown in Fig.4.

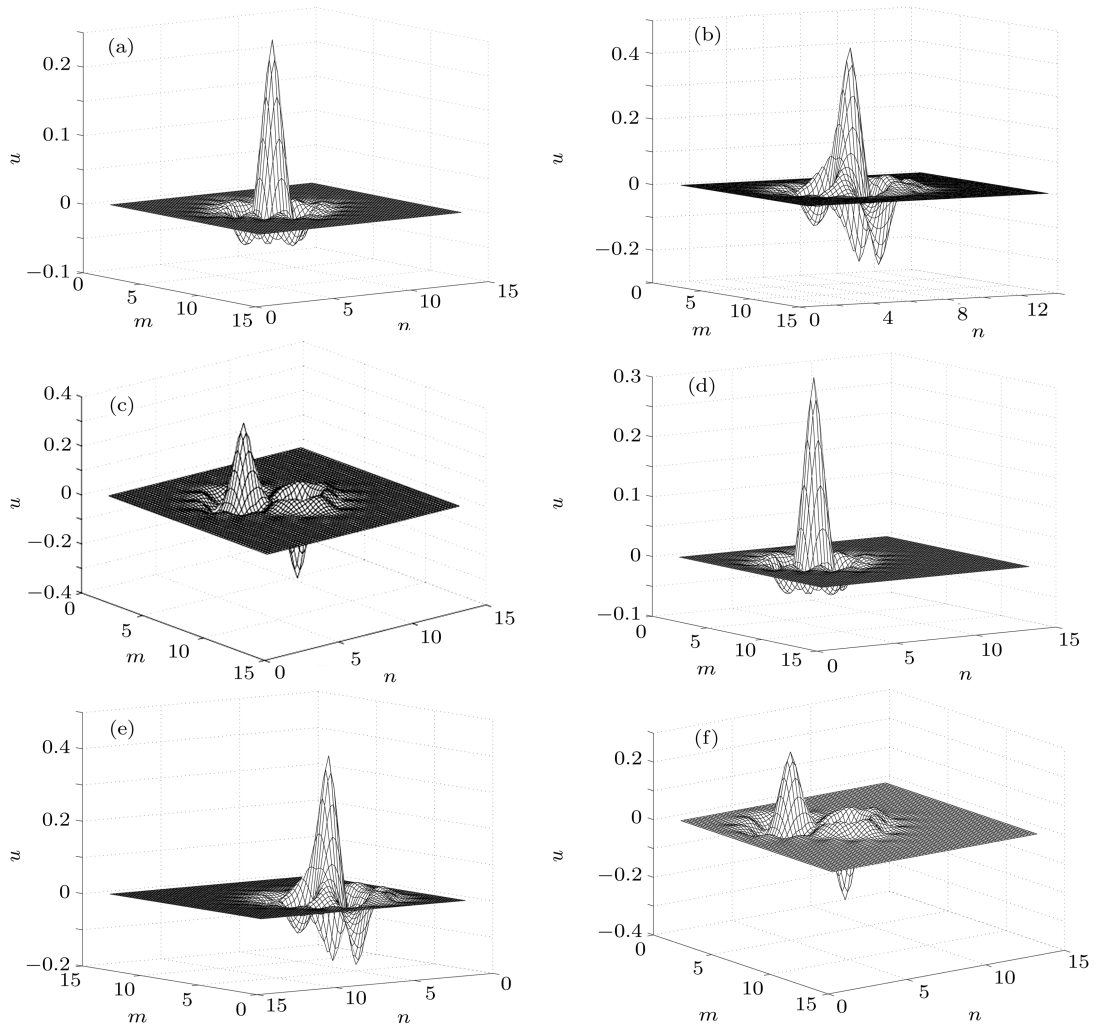


Fig.4. The graphical illustration of the profiles of the 2D DGBS in 2D diatomic KG lattice. (a) The heavy-atom symmetric pattern obtained numerically from Eqs.(16) and (17) with $\gamma = 0.025$, $C = 0.05$, mass ratio $M_1/M_2 = 16$, and breather frequency $\omega = 1.1$. (b) The heavy-atom mirror-symmetric pattern with $\gamma = 0.025$, $C = 0.05$, mass ratio $M_1/M_2 = 16$, and breather frequency $\omega = 1.1$. (c) The heavy-atom asymmetric pattern with $\gamma = 0.025$, $C = 0.05$, mass ratio $M_1/M_2 = 16$, and breather frequency $\omega = 0.5$. (d) The light-atom symmetric pattern with $\gamma = 0.025$, $C = 0.05$, mass ratio $M_1/M_2 = 16$, and breather frequency $\omega = 0.36$. (e) The light-atom mirror-symmetric pattern with $\gamma = 0.025$, $C = 0.05$, mass ratio $M_1/M_2 = 16$, and breather frequency $\omega = 0.36$. (f) The light-atom asymmetric pattern with $\gamma = 0.025$, $C = 0.05$, mass ratio $M_1/M_2 = 16$, and breather frequency $\omega = 0.36$.

According to the numerical result, we see that it is possible to find the 2D DGBs in a 2D KG diatomic face-centered square lattice. The 2D DGBs have the following six cases in symmetries:

Case 1 The 2D DGBs with symmetric profiles are centered at a heavy atom, whether the lattice has a soft or hard nonlinearity, and we call these patterns HS.

Case 2 The 2D DGBs with mirror-symmetric profiles are centered at a heavy atom, whether the lattice has a soft or hard nonlinearity, and we call these patterns HMS.

Case 3 The 2D DGBs with asymmetric profiles are centered at a heavy atom, whether the lattice has a soft or hard nonlinearity, and we call these patterns HA.

Case 4 The 2D DGBs with symmetric profiles are centered at a light atom, whether the lattice has a soft or hard nonlinearity, and we call these patterns LS.

Case 5 The 2D DGBs with mirror-symmetric profiles are centered at a light atom, whether the lattice has a soft or hard nonlinearity, and we call these patterns LMS.

Case 6 The 2D DGBs with asymmetric profiles are centered at a light atom, whether the lattice has a soft or hard nonlinearity, and we call these patterns LA.

The LS, LA, HS and HA patterns have been discussed in 1D β-FPU diatomic chain, but LMS and HMS patterns can only be found in a 2D diatomic face-centered square lattice. This is determined by the structure of the 2D diatomic face-centered square lattice.

In the following, we will discuss the effect of different system parameters on the localisation and stability of DGBs; we only select the HS as an example for analysis.

i) The effect of the different mass ratios on the stability of DGBs (HS)

We have investigated the relation between the mass ratio and stability, the numerical results of Fig.5 show that the mass ratio has only a little effect on the stability of HS patterns in the 2D KG model.

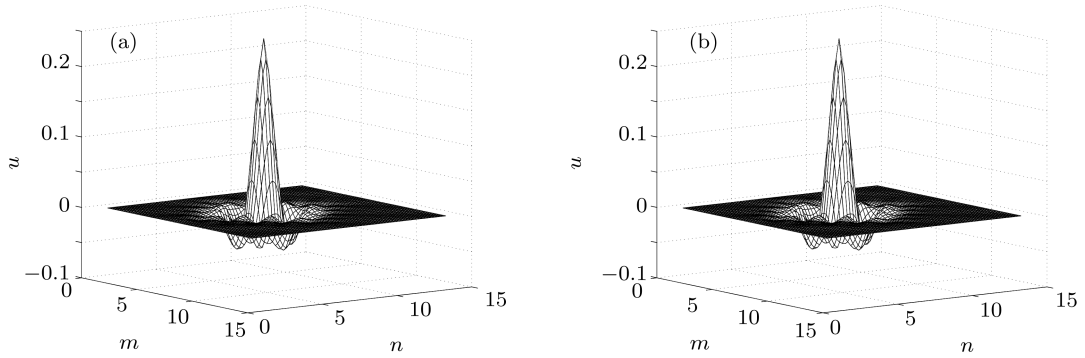


Fig.5. The graphical representation of the effect of different mass ratios on the stability of DGBs (HS), (a) $M_1/M_2 = 2$, (b) $M_1/M_2 = 16$.

ii) The effect of the hard on-site potential or soft on-site potential on the stability of DGBs (HS)

In a 2D KG model, the linear coupling parameter $C > 0$ is attractive coupling, or else repulsive coupling; $\gamma > 0$ is hard on-site potential, or else soft on-site potential. Considering the on-site potential and the type of coupling C, we can conclude that for systems with soft on-site potential, there are no stable DGBs if the coupling between particles is attractive; however, with a repulsive coupling the stability is ensured for fairly high values of the linear coupling parameter C. In Fig.6, we can see that figures 6(a) and 6(b) are stable but figure 6(c) is unstable.

iii) The localization of DGBs (HS) with increasing quartic nonlinear on-site parameter

From the numerical result of Fig.7, we obtain that the 2D DGBs profiles are related closely to the quartic nonlinear on-site parameter: the larger the nonlinear on-site parameter, the larger the amplitude of the 2D DGBs.

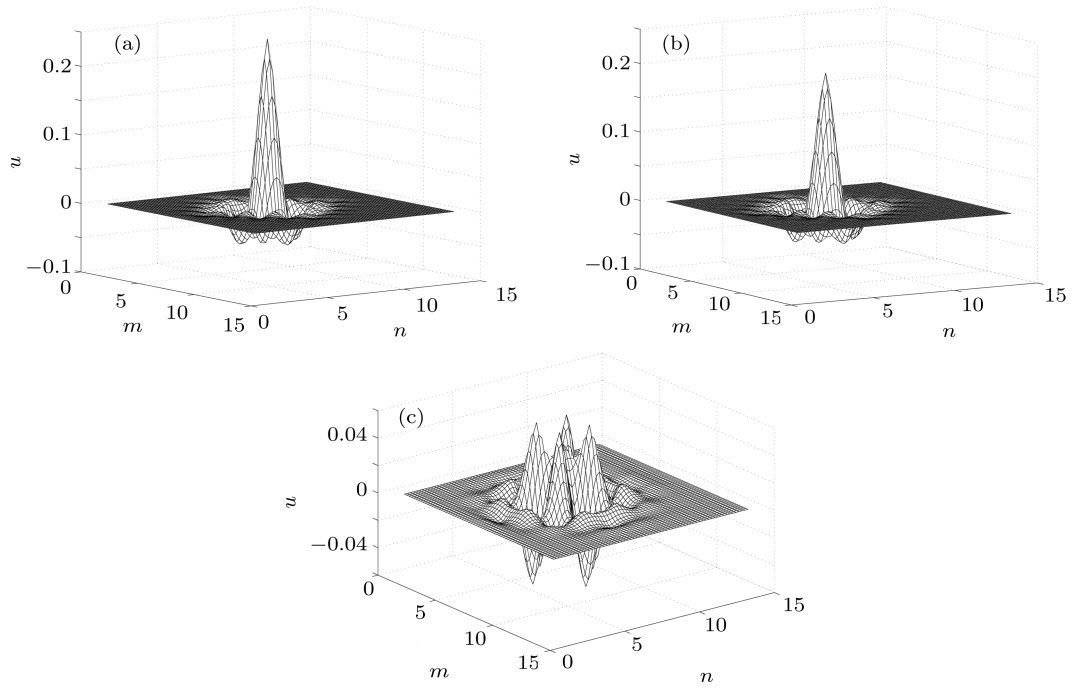


Fig.6. The graphical representation of the profiles of DGBs under different nonlinear on-site potential and coupling potential. (a) Hard on-site potential and attractive coupling with $\gamma = 0.025$ and $C = 0.05$. (b) Soft on-site potential and repulsive coupling with $\gamma = -0.025$ and $C = -0.05$. (c) Hard on-site potential and repulsive coupling with $\gamma = 0.025$ and $C = -0.05$.

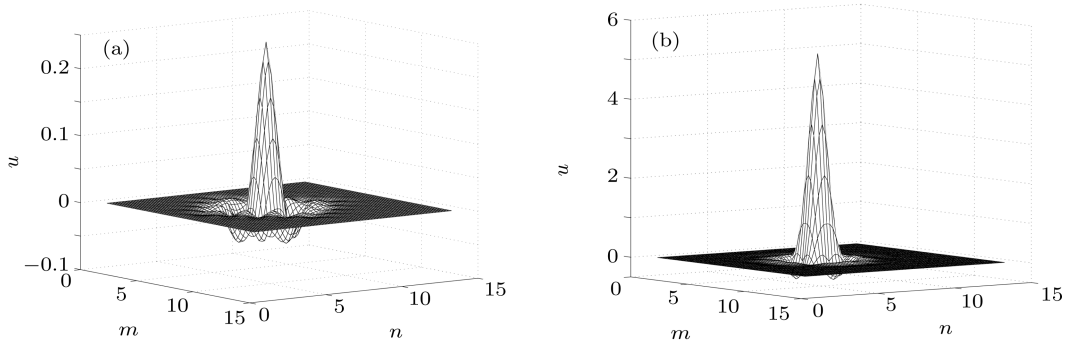


Fig.7. The graphical illustration of the localization of DGBs with increasing nonlinear on-site potential: (a) the small quartic nonlinear on-site potential with $\gamma = 0.025$ and $C = 0.05$, (b) the large quartic nonlinear on-site potential with $\gamma = 5$ and $C = 0.05$.

3.2. The stability of DGBs in two-dimensional KG diatomic face-centered square lattice

The stability of discrete periodic solution of a discrete nonlinear system has been discussed in many papers.[12,16,17] We introduce the variables transformation $u_{2m,2n}(t) \to u_{2m,2n}(t) + \varepsilon_{2m,2n}(t)$, thus the linearized equations of Eqs.(22) and (23) read

$$\begin{aligned} M_1\ddot{\varepsilon}_{2m-1,2n-1} =& -\omega_0^2\varepsilon_{2m-1,2n-1} - \gamma\varepsilon_{2m-1,2n-1}(\varepsilon_{2m-1,2n-1}^2 + 3u_{2m-1,2n-1}\varepsilon_{2m-1,2n-1} + 3u_{2m-1,2n-1}^2) \\ &+ C(\varepsilon_{2m,2n} + \varepsilon_{2m-2,2n-2} + \varepsilon_{2m-2,2n} + \varepsilon_{2m,2n-2} - 4\varepsilon_{2m-1,2n-1}) \\ &+ C(\varepsilon_{2m-1,2n+1} + \varepsilon_{2m-1,2n-3} + \varepsilon_{2m+1,2n-1} + \varepsilon_{2m-3,2n-1} - 4\varepsilon_{2m-1,2n-1}), \qquad (27) \\ M_2\ddot{\varepsilon}_{2m,2n} =& -\omega_0^2\varepsilon_{2m,2n} - \gamma\varepsilon_{2m,2n}(\varepsilon_{2m,2n}^2 + 3u_{2m,2n}\varepsilon_{2m,2n} + 3u_{2m,2n}^2) \\ &+ C(\varepsilon_{2m+1,2n+1} + \varepsilon_{2m-1,2n-1} + \varepsilon_{2m-1,2n+1} + \varepsilon_{2m+1,2n-1} - 4\varepsilon_{2m,2n}) \\ &+ C(\varepsilon_{2m,2n+2} + \varepsilon_{2m,2n-2} + \varepsilon_{2m-2,2n} + \varepsilon_{2m+2,2n} - 4\varepsilon_{2m,2n}), \qquad (28) \end{aligned}$$

where $\varepsilon_{2m,2n}(t)$ and $\varepsilon_{2m-1,2n-1}(t)$ represent the small perturbation of the solution of the dynamical equation. In the following, we only discuss the $\varepsilon_{2m,2n}(t)$ and the analysis of $\varepsilon_{2m-1,2n-1}(t)$ is the same as that of $\varepsilon_{2m,2n}(t)$. The linear stability of these solutions can be studied by finding the eigenvalues of the Floquet matrix F_0, called Floquet multipliers. The Floquet matrix transforms the column matrix with elements given by $\varepsilon_{2m,2n}(t)$ and $\pi(0) \equiv \dot{\varepsilon}_{2m,2n}(0)$ into the corresponding column matrix with elements $\varepsilon_{2m,2n}(T_b)$. And we have $\pi(0) \equiv \dot{\varepsilon}_{2m,2n}(0)$ and $T_b = 2\pi/\omega_b$, that is

$$\begin{pmatrix} \{\varepsilon_{2m,2n}(T_b)\} \\ \{\pi_{2m,2n}(T_b)\} \end{pmatrix} = F_0 \begin{pmatrix} \{\varepsilon_{2m,2n}(0)\} \\ \{\pi_{2m,2n}(0)\} \end{pmatrix}. \tag{29}$$

The Floquet matrix F_0 can be obtained by choosing zero initial conditions except for one position or momentum equal to unity, and intergrating Eq.(28) numerically in a time span of a breather period. The final positions and momentum give the elements of the corresponding column of the Floquet matrix. In order to obtain accurate results, we have used a symplectic integrator. Equation (28) can be written as an eigenvalue equation

$$(N(u(t), \xi) \bullet \varepsilon)_{2m,2n} = E\varepsilon_{2m,2n}, \tag{30}$$

where $N(u(t), \xi)$ is called Newton operator. The solutions of Eq.(28) can be described as the eigenfunctions of Newton operator for $E = 0$. The fact that the linearized system is Hamiltonian and real implies that the Floquet operator is a real and symplectic operator. The consequence is that if λ is an eigenvalue, then $1/\lambda$, λ^* and $1/\lambda^*$ are also eigenvalues, and therefore a necessary condition for linear stability is that every eigenvalue has its modulus equal to one, i.e. it is located in the unit circle on the complex plane. When the coupling C is switched on, the eigenvalue moves on the complex plane as a continuous function of C, and an instability can be produced only in three different ways:[17]

a) A couple of conjugate eigenvalues reaches the value $1+0\,\mathrm{i}$ ($\theta = 0$) and leaves the unit circle along the real line (harmonic bifurcation);

b) A couple of conjugate eigenvalues reaches –1 ($\theta = \pm\pi$) and leaves the unit circle along the real line (subharmonic bifurcation);

c) Two pairs of conjugate eigenvalues collide at two conjugate points in the unit circle and leave it (Kreign crunch or oscillatory bifurcation).

The study of breather stability can be complemented by means of Aubry's band theory. It consists of studying the linearized system (29) for $E \neq 0$, with the corresponding family of Floquet operators F_E. For each operator F_E there are $2 \times N$ Floquet multipliers. A Floquet multiplier can be written as $\lambda = \exp(\mathrm{i}\theta)$, θ is called the Floquet argument. If θ is real then $|\exp(\mathrm{i}\theta)| = 1$ and the corresponding eigenfunction of Eq.(29) is bounded and corresponds to a stability mode. If θ is complex, it corresponds to an instability mode. The set of points (θ, E) with θ real, has a band structure. The breather is stable if there are $2 \times N$ band intersections with the axis $E = 0$. If the on-site potential is soft, the band will be tangent to the $E = 0$ axis at (0, 0) with positive curvature. When the coupling is switched on and is an attractive potential, the bands move upwards, and the intersection points disappear, which implies that some Floquet arguments become complex or, equivalently, that some Floquet multipliers abandon the unit circle and the breather becomes unstable.

In this paper, we use Aubry's band analysis and obtain some conclusions about the stability of DGBs in a 2D KG diatomic face-centered square lattice.

(I) In this system, considering the on-site potential and the type of coupling, we obtain that for systems with soft on-site potential, there are no stable DGBs if the coupling between particles is attractive, but with a repulsive coupling the stability is ensured for fairly high values of the coupling parameter C.

(II) For systems with hard on-site potentials, the situation is opposite and the DGBs are stable with attractive coupling and unstable with repulsive coupling.

(III) In the system, we only consider the on-site potential being symmetric ($\kappa = 0$), this characteristic enlarges the stability range.

The reason why the system with hard on-site potential and repulsive coupling is unstable, is that further increase of C will lead to harmonic bifurcation; this instability mode is an asymmetric-extended one. For the system with soft-on site and attractive coupling, since no subharmonic bifurcations at $\lambda = \pm 1$ occur, the bands are gapless at $\theta = \pm\pi$. The system eventually becomes unstable through harmonic bifurcations. The difference, when we consider the second nearest-neighbour interaction, is that we can obtain more accurate numerical solutions and stability of breathers. In a 2D model, the second nearest-neighbour interaction is too strong to be ignored, so it is necessary to consider this interaction.

3.3. The discrete gap breathers in a 2D β-FPU diatomic face-centered square lattice

For $\omega_0 = \kappa = \gamma = \alpha = 0$, the model is of a 2D β-FPU diatomic face-centered square lattice. By taking into account the interaction between the lattice and its nearest-neighbors, the Hamiltonian of the 2D β-FPU face-centered square lattice is given by

$$\begin{aligned} H = \sum_{m,n} \Bigg[& \frac{\dot{u}^2_{2m-1,2n-1}}{2M_1} + \frac{\dot{u}^2_{2m,2n}}{2M_2} + \frac{1}{2}C\left(u_{2m,2n} - u_{2m-1,2n-1}\right)^2 + \frac{1}{2}C\left(u_{2m+1,2n+1} - u_{2m,2n}\right)^2 \\ & + \frac{1}{2}\beta\left(u_{2m,2n} - u_{2m-1,2n-1}\right)^4 + \frac{1}{2}\beta\left(u_{2m+1,2n+1} - u_{2m,2n}\right)^4 \Bigg], \end{aligned} \tag{31}$$

where M_1 and M_2 are the masses of the heavy and light atoms, $u_{2m-1,2n-1}$ and $u_{2m,2n}$ are the displacements of the heavy and light atoms in the (m,n)-th cell of the lattice from their equilibriums, C and β are the linear and nonlinear coupling parameters, respectively. The nonlinear vibration equations for this system are obtained as follows:

$$\begin{aligned} M_1\ddot{u}_{2m-1,2n-1} = & C\left(u_{2m,2n} + u_{2m-2,2n-2} + u_{2m-2,2n} + u_{2m,2n-2} - 4u_{2m-1,2n-1}\right) \\ & + \beta\Big[\left(u_{2m,2n} - u_{2m-1,2n-1}\right)^3 - \left(u_{2m-1,2n-1} - u_{2m-2,2n-2}\right)^3 + \left(u_{2m,2n-2} - u_{2m-1,2n-1}\right)^3 \\ & - \left(u_{2m-1,2n-1} - u_{2m-2,2n}\right)^3\Big], \end{aligned} \tag{32}$$

$$\begin{aligned} M_2\ddot{u}_{2m,2n} = & C\left(u_{2m+1,2n+1} + u_{2m-1,2n-1} + u_{2m-1,2n+1} + u_{2m+1,2n-1} - 4u_{2m,2n}\right) \\ & + \beta\Big[\left(u_{2m+1,2n+1} - u_{2m,2n}\right)^3 - \left(u_{2m,2n} - u_{2m-1,2n-1}\right)^3 + \left(u_{2m+1,2n-1} - u_{2m,2n}\right)^3 \\ & - \left(u_{2m,2n} - u_{2m-1,2n+1}\right)^3\Big]. \end{aligned} \tag{33}$$

The linear dispersive relation of the phonon of the lattice is as follows:

$$\omega^2 = \frac{C}{M_1M_2}\left[(M_1 + M_2) \pm \sqrt{M_1^2 + M_2^2 + 2M_1M_2\cos 4qa_0}\right], \tag{34}$$

where the sign "–" ("+") stands for the acoustic (optical) phonon band.

We define the edges of these bands by ω_1, ω_2, ω_3 and ω_4, thus we have

$$\begin{aligned} & \omega_1 = 0, \quad (q \to 0), \quad \omega_2 = \sqrt{\frac{2C}{M_1}}, \quad \left(q = \pm\frac{\pi}{4a_0}\right), \\ & \omega_3 = \sqrt{\frac{2C}{M_2}}, \quad \left(q = \pm\frac{\pi}{4a_0}\right), \quad \omega_4 = \sqrt{\frac{2C}{\mu}}, \quad (q \to 0), \end{aligned} \tag{35}$$

where $\mu = M_1M_2/(M_1 + M_2)$ and $M_1 > M_2$. The acoustic band has the frequencies lying between ω_1 and ω_2, and the optical one has the frequencies lying between ω_3 and ω_4. We call ω_2 and ω_3 the lower and the upper edges of the phonon band gap, respectively.

In the above analysis, we only consider the nearest-neighbour interactions. In the 2D system, the second nearest-neighbour interaction is also important for the stability of system. In the following, we analyse the stability of the 2D DGBs by considering the nearest-neighbour and the second nearest-neighbour interactions. The nonlinear vibration equation for this system is obtained as follows:

$$\begin{aligned} & M_1\ddot{u}_{2m-1,2n-1} \\ = & C\left(u_{2m,2n} + u_{2m-2,2n-2} + u_{2m-2,2n} + u_{2m,2n-2} - 4u_{2m-1,2n-1}\right) \\ & + C\left(u_{2m-1,2n+1} + u_{2m-1,2n-3} + u_{2m+1,2n-1} + u_{2m-3,2n-1} - 4u_{2m-1,2n-1}\right) \\ & + \beta\Big[\left(u_{2m,2n} - u_{2m-1,2n-1}\right)^3 - \left(u_{2m-1,2n-1} - u_{2m-2,2n-2}\right)^3 + \left(u_{2m,2n-2} - u_{2m-1,2n-1}\right)^3 \\ & - \left(u_{2m-1,2n-1} - u_{2m-2,2n}\right)^3\Big] + \beta\Big[\left(u_{2m-1,2n+1} - u_{2m-1,2n-1}\right)^3 - \left(u_{2m-1,2n-1} - u_{2m-1,2n-3}\right)^3 \\ & + \left(u_{2m+1,2n-1} - u_{2m-1,2n-1}\right)^3 - \left(u_{2m-1,2n-1} - u_{2m-3,2n-1}\right)^3\Big], \end{aligned} \tag{36}$$

$$
\begin{aligned}
& M_1\ddot{u}_{2m,2n} \\
= & C\left(u_{2m+1,2n+1}+u_{2m-1,2n-1}+u_{2m-1,2n+1}+u_{2m+1,2n-1}-4u_{2m,2n}\right) \\
& + C\left(u_{2m,2n+2}+u_{2m,2n-2}+u_{2m-2,2n}+u_{2m-2,2n}-4u_{2m,2n}\right) \\
& + \beta\left[\left(u_{2m+1,2n+1}-u_{2m,2n}\right)^3-\left(u_{2m,2n}-u_{2m-1,2n-1}\right)^3+\left(u_{2m+1,2n-1}-u_{2m,2n}\right)^3\right. \\
& \left. - \left(u_{2m,2n}-u_{2m-1,2n+1}\right)^3\right]+\beta\left[\left(u_{2m,2n+2}-u_{2m,2n}\right)^3-\left(u_{2m,2n}-u_{2m,2n-2}\right)^3\right. \\
& \left. + \left(u_{2m+2,2n}-u_{2m,2n}\right)^3-\left(u_{2m,2n}-u_{2m-2,2n}\right)^3\right], \qquad (37)
\end{aligned}
$$

In numerical calculation, a necessary condition for the breathers to exist is to avoid resonances with the phonons, i.e. the breather frequency and all its higher harmonics should be outside the phonon bands. The frequency, however, can lie inside the gap or above the optical band. Here, we only focus on the case that it lies inside the gap. For this, we introduce the LAA and RWA, and still assume the 2D DGBs to be of the types given in Eq.(24).

Substituting Eq.(24) into Eqs.(36) and (37) separately yields

$$
\begin{aligned}
& \left(\frac{\omega^2}{\omega_2^2}-2\right)u^0_{2m-1,2n-1}+\frac{1}{2}\left(u^0_{2m,2n}+u^0_{2m-2,2n-2}+u^0_{2m-2,2n}+u^0_{2m,2n-2}-2u^0_{2m-1,2n-1}\right) \\
& + \frac{1}{2}\left(u^0_{2m-1,2n+1}+u^0_{2m-1,2n-3}+u^0_{2m+1,2n-1}+u^0_{2m-3,2n-1}-2u^0_{2m-1,2n-1}\right) \\
& + \frac{\beta}{4C}\left[\left(u^0_{2m,2n}-u^0_{2m-1,2n-1}\right)^3-\left(u^0_{2m-1,2n-1}-u^0_{2m-2,2n-2}\right)^3+\left(u^0_{2m,2n-2}-u^0_{2m-1,2n-1}\right)^3\right. \\
& \left. - \left(u^0_{2m-1,2n-1}-u^0_{2m-2,2n}\right)^3\right]+\frac{\beta}{4C}\left[\left(u^0_{2m-1,2n+1}-u^0_{2m-1,2n-1}\right)^3-\left(u^0_{2m-1,2n-1}-u^0_{2m-1,2n-3}\right)^3\right. \\
& \left. + \left(u^0_{2m+1,2n-1}-u^0_{2m-1,2n-1}\right)^3-\left(u^0_{2m-1,2n-1}-u^0_{2m-3,2n-1}\right)^3\right]=0, \qquad (38) \\
& \left(\frac{\omega^2}{\omega_3^2}-2\right)u^0_{2m,2n}+\frac{1}{2}\left(u^0_{2m+1,2n+1}+u^0_{2m-1,2n-1}+u^0_{2m-1,2n+1}+u^0_{2m+1,2n-1}-2u^0_{2m,2n}\right) \\
& + \frac{1}{2}\left(u^0_{2m,2n+2}+u^0_{2m,2n-2}+u^0_{2m-2,2n}+u^0_{2m+2,2n}-2u^0_{2m,2n}\right) \\
& + \frac{\beta}{4C}\left[\left(u^0_{2m+1,2n+1}-u^0_{2m,2n}\right)^3-\left(u^0_{2m,2n}-u^0_{2m-1,2n-1}\right)^3+\left(u^0_{2m+1,2n-1}-u^0_{2m,2n}\right)^3\right. \\
& \left. - \left(u^0_{2m,2n}-u^0_{2m-1,2n+1}\right)^3\right]+\frac{\beta}{4C}\left[\left(u^0_{2m,2n+2}-u^0_{2m,2n}\right)^3-\left(u^0_{2m,2n}-u^0_{2m,2n-2}\right)^3\right. \\
& \left. + \left(u^0_{2m+2,2n}-u^0_{2m,2n}\right)^3-\left(u^0_{2m,2n}-u^0_{2m-2,2n}\right)^3\right]=0. \qquad (39)
\end{aligned}
$$

Applying the same numerical methods to the 2D KG model, we find that in a 2D FPU model there are also six kinds of DGBs, as in the 2D KG model. The different system parameters have different effects on the 2D DGBs. In the following, we will analyse the different effects on the DGBs by numerical calculation.

I) The effect of different mass ratios on the stability of DGBs (HS)

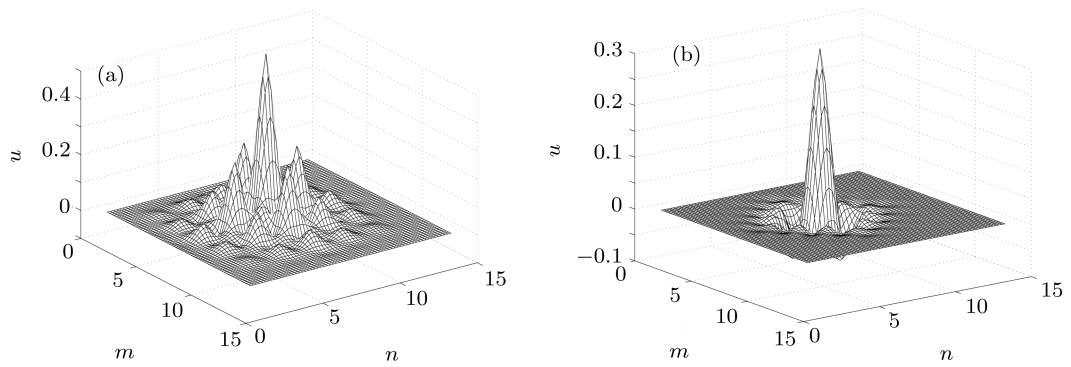


Fig.8. The graphical representation of the effect of different mass ratios on the stability of DGBs, (a) $M_1/M_2=2$; (b) $M_1/M_2=16$.

From the numerical results of Fig.8, we obtain that the 2D DGBs profiles are related closely to the mass ratio, i.e., the larger the mass ratio, the better the localization of the 2D DGBs profiles. This is because the interaction of the neaest-neighbouring atoms in the 2D diatomic FPU models becomes weaker when the mass ratio increases.

II) The effect of the hard coupling potential or soft coupling potential on the stability of DGBs (HS)

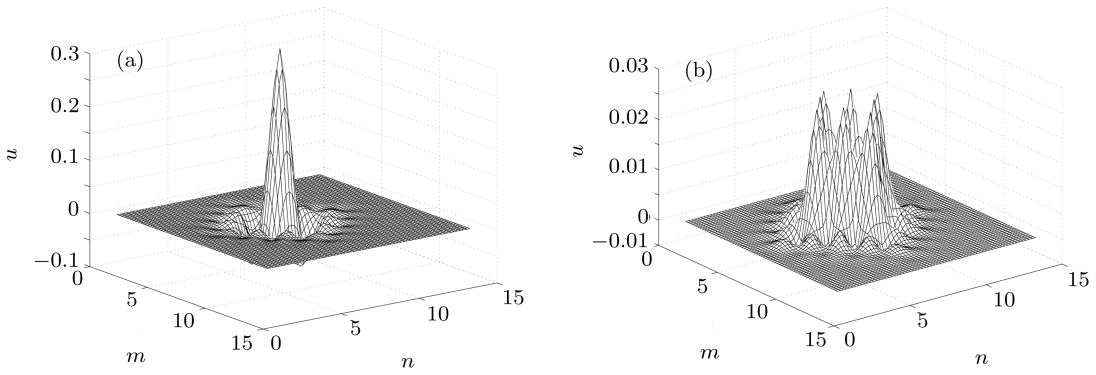


Fig.9. The graphical representation of the profiles of the effect of different nonlinear coupling potentials. (a) Hard coupling potential with $C = 0.05$, $\beta = 0.025$, mass ratio $M_1/M_2 = 16$, and breather frequency $\omega = 1.1$. (b) Soft coupling potential with $C = 0.05$, $\beta = -0.025$, mass ratio $M_1/M_2 = 16$, and breather frequency $\omega = 1.1$.

In a 2D FPU model, there is no on-site potential. The nonlinear coupling parameter $\beta > 0$ is the hard coupling potential, and otherwise $\beta < 0$ is the soft coupling potential. We have also investigated the relation between the coupling potential and stability. The numerical results of Fig.9 show that for the hard coupling potential, the localisation of the 2D DGBs profiles is better than that for the soft coupling potential.

III) The localisation of DGBs (HS) with increasing quartic nonlinear coupling parameter

From the numerical results of Fig.10, we obtain that the 2D DGBs profiles are related closely to the quartic nonlinear coupling parameter: the larger the nonlinear coupling parameters, the larger the amplitude of the 2D DGBs.

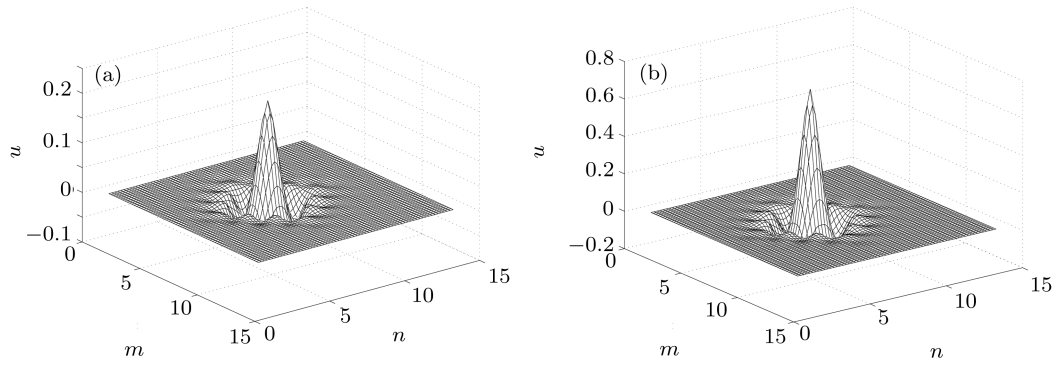


Fig.10. The graphical illustration of the localization of DGBs with increasing nonlinear coupling potential; (a) the small quartic nonlinear coupling potential with $\beta = 0.005$ (b) the large quartic nonlinear coupling potential with $\beta = 0.1$.

3.4. The stability of DGBs in two-dimensional β-FPU diatomic face-centered square lattice

Next, we discuss the stability of these solutions. According to Aubry's theory, if we introduce the variable transformations $u_{2m-1,2n-1}(t) \to u_{2m-1,2n-1}(t) + \varepsilon_{2m-1,2n-1}(t)$ and $u_{2m,2n}(t) \to u_{2m,2n}(t) + \varepsilon_{2m,2n}(t)$, equations (36) and (37) become, respectively,

$M_1\ddot{\varepsilon}_{2m-1,2n-1}$

$$
\begin{aligned}
&= C(\varepsilon_{2m,2n} + \varepsilon_{2m-2,2n-2} + \varepsilon_{2m-2,2n} + \varepsilon_{2m,2n-2} - 4\varepsilon_{2m-1,2n-1}) \\
&\quad + C(\varepsilon_{2m-1,2n+1} + \varepsilon_{2m-1,2n-3} + \varepsilon_{2m+1,2n-1} + \varepsilon_{2m-3,2n-1} - 4\varepsilon_{2m-1,2n-1}) \\
&\quad + \beta[(u_{2m,2n} - u_{2m-1,2n-1})^2(\varepsilon_{2m,2n} - \varepsilon_{2m-1,2n-1}) + (u_{2m-1,2n-1} - u_{2m-2,2n-2})^2(\varepsilon_{2m-1,2n-1} - \varepsilon_{2m-2,2n-2}) \\
&\quad + (u_{2m,2n-2} - u_{2m-1,2n-1})^2(\varepsilon_{2m,2n-2} - \varepsilon_{2m-1,2n-1}) + (u_{2m-1,2n-1} - u_{2m-2,2n})^2(\varepsilon_{2m-1,2n-1} - \varepsilon_{2m-2,2n})] \\
&\quad + \beta[(u_{2m-1,2n+1} - u_{2m-1,2n-1})^2(\varepsilon_{2m-1,2n+1} - \varepsilon_{2m-1,2n-1}) - (u_{2m-1,2n-1} - u_{2m-1,2n-3})^2 \\
&\quad \times (\varepsilon_{2m-1,2n-1} - \varepsilon_{2m-1,2n-3}) + (u_{2m+1,2n-1} - u_{2m-1,2n-1})^2(\varepsilon_{2m+1,2n-1} - \varepsilon_{2m-1,2n-1}) \\
&\quad - (u_{2m-1,2n-1} - u_{2m-3,2n-1})^2(\varepsilon_{2m-1,2n-1} - \varepsilon_{2m-3,2n-1})], \qquad (40)
\end{aligned}
$$

$$
\begin{aligned}
&M_2\ddot{\varepsilon}_{2m,2n} \\
&= C(\varepsilon_{2m+1,2n+1} + \varepsilon_{2m-1,2n-1} + \varepsilon_{2m-1,2n+1} + \varepsilon_{2m+1,2n-1} - 4\varepsilon_{2m,2n}) \\
&\quad + C(\varepsilon_{2m,2n+2} + \varepsilon_{2m,2n-2} + \varepsilon_{2m-2,2n} + \varepsilon_{2m+2,2n} - 4\varepsilon_{2m,2n}) \\
&\quad + \beta[(u_{2m+1,2n+1} - u_{2m,2n})^2(\varepsilon_{2m+1,2n+1} - \varepsilon_{2m,2n}) + (u_{2m,2n} - u_{2m-1,2n-1})^2(\varepsilon_{2m,2n} - \varepsilon_{2m-1,2n-1}) \\
&\quad + (u_{2m+1,2n-1} - u_{2m,2n})^2(\varepsilon_{2m+1,2n-1} - \varepsilon_{2m,2n}) + (u_{2m,2n} - u_{2m-1,2n+1})^2(\varepsilon_{2m,2n} - \varepsilon_{2m-1,2n+1})] \\
&\quad + \beta[(u_{2m,2n+2} - u_{2m,2n})^2(\varepsilon_{2m,2n+2} - \varepsilon_{2m,2n}) - (u_{2m,2n} - u_{2m,2n-2})^2(\varepsilon_{2m,2n} - \varepsilon_{2m,2n-2}) \\
&\quad + (u_{2m+2,2n} - u_{2m,2n})^2(\varepsilon_{2m+2,2n} - \varepsilon_{2m,2n}) - (u_{2m,2n} - u_{2m-2,2n})^2(\varepsilon_{2m,2n} - \varepsilon_{2m-2,2n})], \qquad (41)
\end{aligned}
$$

where $\varepsilon_{2m-1,2n-1}$ and $\varepsilon_{2m,2n}$ represent the small perturbation in the solution of the dynamical equations. If no solutions of Eqs.(40) and (41) diverge exponentially for a very long time, the solutions of Eqs.(36) and (37) are said to be linearly stable. This property does not imply that a perturbation in the initial conditions will remain small for all time for the real nonlinear dynamical system (31). However, this linear stability implies that disturbance will not grow exponentially with increasing time. Such trajectories have physically a significantly longer life-time than those linearly unstable.

According to Aubry's theory,[17] the linear stability of the breather solution depends on whether the eigenvalues of the Floquet matrix equal 1, or a small perturbation of the solution will not grow exponentially with increasing time. Since the Floquet matrix is symplectic, a breather is stable only if all the eigenvalues of the Floquet matrix lie in the unit circle. The Floquet stability analysis of all these patterns showed that only HA mode is unstable for all the gap frequencies. This instability comes from the fact that HA mode is a multi-breather, centered at a heavy atom at rest, with its nearest-neighbour light atoms oscillating out of phase. In physics terms, the heavy atoms strongly perturb the motion of the light atoms which are easily drawn into the oscillating motion. We also investigated the relation between the mass ratio and stability; the results show that the stability of HS and LS patterns will become worse when the mass ratio decreases. This instability comes from the fact that the light atoms of these modes are perturbed more so than the motion of the heavy atoms, while the mass ratio between the heavy atom and the light atom decreases. However, the changing of the mass ratio does not strongly affect the stability of HMS, HA, LMS and LA patterns; the reason may be that the centered atoms of these modes are at rest, and the directions that the nearest-neighbouring atoms act on the centered atoms are opposite to each other.

4. Conclusions

In this paper, we have studied a general 2D diatomic face-centered square lattice with on-site and coupling potentials separately. The model covers a lot of 2D diatomic systems, so this model can be transformed into the 2D diatomic KG and the 2D diatomic FPU systems, or other systems. In the harmonic approximation, we discussed the linear dispersive relation of the phonon of the 2D diatomic KG and 2D diatomic FPU lattices. At the same time, we also discussed the different system parameters that have different effects on the localization of the 2D DGBs. After that, we investigated the possibility of the existence and stability of the 2D DGBs in a 2D diatomic face-centered square lattice. We proved their existence by using RWA, LAA and the numerical method, and obtained six types of 2D DGBs, i.e., symmetric,

mirror-symmetric and asymmetric, no matter whether the center of the breather lies on a light or a heavy atom. In the 2D KG diatomic face-centered square lattice, by using Aubry's band analysis, we gave the conditions of the stabilities of the DGBs in the systems, i.e. the systems with soft on-site potential. There are no stable DGBs if the coupling between particles is attractive, but for a repulsive coupling the stability is ensured for fairly high values of the linear coupling parameter C. The conclusions are consistent with the result obtained by numerical calculation as shown in Fig.6. In the 2D β-FPU diatomic face-centered square lattice, according to Aubry's theory, only HA mode is unstable for all the gap frequencies. We also investigated the relation between the mass ratio and stability, the results show that the stability of HS and LS patterns will become worse when the mass ratio decreases. This instability comes from the fact that the light atoms of these modes are perturbed more strongly than the motion of the heavy atoms, while the mass ratio between the heavy atom and the light atom decreases. In this article by discussing the DGBs in 1D and 2D systems, we attained the difference between them. The main difference is that there are four types of DGBs (HS, LS, HA, LA) in 1D diatomic chain. However, there are six types of DGBs (HS, HMS, HA, LS, LMS, LA) in 2D diatomic lattice. The same characteristics are shown in both the systems that the larger the mass ratio, the better the localization of the DGBs profiles; and the larger the nonlinear parameters, the larger the amplitudes of the DGBs.

References

[1] Sievers A J and Takeno S 1988 *Phys. Rev. Lett.* **61** 970
[2] Page J B 1991 *Phys. Rev.* B **41** 7835
[3] Mackay R S and Aubry S 1994 *Nonlinearity* **7** 1623
[4] Cretegny T, Livi R and Spicci M 1998 *Physica* D **119** 88
[5] Maniadis P, Zolotaryuk A V and Tsironis G P 2003 *Phys. Rev.* E **67** 046612
[6] James G and Noble P 2004 *Physica* D **196** 124
[7] Li M S and Tian Q 2007 *Acta Phys. Sin.* **56** 1401 (in Chinese)
[8] Zhou Q, Lü B B and Tian Q 2009 *Acta Phys. Sin.* **58** 411 (in Chinese)
[9] Lü B B, Zhou Q and Tian Q 2008 *Journal of Beijing Normal University* (Natureal Science) **44** 476 (in Chinese)
[10] Lü B B and Tian Q 2008 *Journal of Beijing Normal University* (Natureal Science) **44** 581 (in Chinese)
[11] Butt I A and Wattis J A D 2006 *J. Phys.* A: *Math. Gen.* **39** 4955
[12] Bao F F and Takuji K 2007 *Wave Motion* **45** 68
[13] Mackay R S and Aubry S 1994 *Nonlinearity* **7** 1623
[14] Aubry S 1994 *Physica* D **71** 196
[15] Aubry S 1995 *Physica* D **86** 248
[16] Marin J L and Aubry S 1996 *Nonlinearity* **9** 1501
[17] Aubry S 1997 *Physica* D **103** 201
[18] Marin J L, Aubry S and Floria L M 1998 *Physica* D **113** 283